

Certified Per-Instance Unlearning Using Individual Sensitivity Bounds

Hanna Benarroch^{*1}, Jamal Atif², and Olivier Cappé¹

¹DI ENS, École normale supérieure, Université PSL, CNRS, 75005 Paris, France

²CMAP, École polytechnique, Institut Polytechnique de Paris, 91120 Palaiseau, France

Abstract

Certified machine unlearning can be achieved via noise injection leading to differential privacy guarantees, where noise is calibrated to worst-case sensitivity. Such conservative calibration often results in performance degradation, limiting practical applicability. In this work, we investigate an alternative approach based on adaptive per-instance noise calibration tailored to the individual contribution of each data point to the learned solution. This raises the following challenge: *how can one establish formal unlearning guarantees when the mechanism depends on the specific point to be removed?* To define individual data point sensitivities in noisy gradient dynamics, we consider the use of per-instance differential privacy. For ridge regression trained via Langevin dynamics, we derive high-probability per-instance sensitivity bounds, yielding certified unlearning with substantially less noise injection. We corroborate our theoretical findings through experiments in linear settings and provide further empirical evidence on the relevance of the approach in deep learning settings.

1 Introduction

Modern machine learning systems increasingly operate under regulatory and contractual constraints that require the *post-hoc* removal of individual training examples, for instance in the context of the “right to be forgotten” (Marino et al., 2025). The gold standard is to retrain the model from scratch on the dataset with the target example removed, but such retraining is often computationally infeasible in practice. Machine unlearning seeks to approximate the effect of retraining at a substantially lower cost, either by enforcing exact equivalence with retraining (*exact unlearning*) (Cao and Yang, 2015) or by matching the retrained

model only in distribution (*approximate unlearning*) (Ginart et al., 2019; Sekhari et al., 2021). We focus on *approximate unlearning*.

We further restrict attention to *certified* unlearning, where deletion procedures are accompanied by explicit, provable guarantees. Such guarantees are naturally connected to differential privacy (DP), which quantifies how the output distribution of a randomized mechanism changes when a single training point is removed. While DP provides a natural language for reasoning about certified deletion, its guarantees do not directly transfer to the unlearning setting.

A first mismatch concerns the notion of adjacency. Differential privacy allows either removing or substituting a data point, whereas unlearning compares training to retraining the model as if a given point had never been part of the dataset. Substitution-based adjacency therefore lacks a natural interpretation for unlearning, although it is sometimes used for technical convenience (e.g., Chien et al., 2024).

The most important difference, however, lies in the nature of the guarantee itself. Differential privacy certifies a mechanism *a priori*, uniformly over all datasets and all data points. Unlearning, by contrast, is inherently *post-hoc*: it targets a specific trained model, a specific dataset, and a specific data point whose deletion is requested.

First, this post-hoc nature affects how unlearning guarantees should be defined. While many existing approaches compare unlearning to a full retraining oracle (Ginart et al., 2019; Neel et al., 2021; Guo et al., 2020; Koloskova et al., 2025; Mu and Klabjan, 2025), we follow several recent works (Lu et al., 2025; Basaran et al., 2025; Waerebeke et al., 2025) and adopt a *self-referenced* notion of unlearning, which compares two executions of the same unlearning procedure on adjacent datasets. This isolates what is certified intrinsically by the unlearning mechanism.

Second, this conceptual difference affects how guarantees should be calibrated across data points. Uni-

^{*}Corresponding author: hanna.benarroch@ens.psl.eu

form DP guarantees, while stronger in generality, enforce an homogeneous treatment of all data points, regardless of their actual influence on the learned model. This regime is implicitly adopted by some certified unlearning approaches, including Langevin-based methods (Chien et al., 2024). In contrast, we argue that certified unlearning should explicitly exploit the fact that deletion targets a specific dataset and a specific data point. This naturally calls for *per-instance* certified unlearning, where guarantees are calibrated to the actual influence of the point being removed, avoiding unnecessary addition of noise and loss of utility. This view is supported by recent work on individualized guarantees (Sepahvand et al., 2025) and by empirical evidence showing that worst-case sensitivity bounds often overestimate the influence of typical data points (Thudi et al., 2024).

We now turn to the practical question of how to derive certified unlearning guarantees within this framework. As in (Chien et al., 2024), we consider unlearning procedures based on Langevin dynamics. Our analysis builds on recent results by Bok et al. (2024), who show how privacy loss can be tracked along noisy optimization trajectories during learning. We extend this reasoning to the *learn-then-unlearn* setting, where the learning noise is fixed and certified deletion guarantees are obtained by calibrating the additional noise injected during unlearning to reach a target privacy level.

We then examine how this analysis can be refined at the level of individual data points. To this end, we introduce *per-instance sensitivity* as the central quantity and use it to derive certified guarantees for approximate unlearning. In the case of ridge regression trained with Langevin dynamics, we show that although sensitivities are formally unbounded due to the Gaussian nature of the iterates, they can be sharply controlled with high probability and evaluated efficiently. This yields certified unlearning guarantees that adapt to the actual influence of the removed data point, rather than relying on a worst-case bound.

Overall, our results show that the *difficulty of unlearning is not uniform*. Data points that exert little influence on the training dynamics are inherently easier to forget and require less noise to certify their deletion, a phenomenon we analyze theoretically in the linear setting and observe empirically beyond it.

Our contributions can be summarized as follows:

- We adapt the shifted interpolation framework of Bok et al. (2024) to the learn-then-unlearn setting, enabling per-instance certified unlearning.
- We derive sharp high-probability per-instance sensitivity bounds for ridge regression un-

der Langevin dynamics, yielding heterogeneous unlearning guarantees and improved privacy-accuracy trade-offs compared to uniform calibration.

- We provide empirical evidence of similar instance-level heterogeneity in a typical deep learning setting, despite the lack of a supporting theoretical analysis.

2 Related work

Exact and approximate unlearning. Early work on machine unlearning focused on *exact* deletion, requiring the post-deletion model to coincide with retraining on the dataset with the removed point (Cao and Yang, 2015) (e.g., Remark 4.5). Such guarantees rely on strong structural assumptions and do not scale to modern learning pipelines. This motivated the probabilistic formulation introduced by Ginart et al. (2019), which requires the output distribution of an unlearning algorithm to be close to that of retraining. Our work adopts this probabilistic viewpoint.

Gradient-based unlearning with noisy optimization. Most unlearning methods involve further optimization steps that exclude the data point to be forgotten. Descent-to-Delete (Neel et al., 2021) performs additional gradient descent steps followed by output perturbation to obtain privacy guarantees. However, as shown by Chien et al. (2024), this approach leads to more conservative noise calibration than injecting noise at each gradient step. Building on this insight, they proposed a Langevin-based unlearning procedure analyzed under uniform sensitivity bounds and implementing deletion via a replacement-based mechanism. Our work follows the same noisy-gradient paradigm but differs by considering omission-based unlearning, and by calibrating the noise in an instance-dependent way.

Per-instance unlearning mechanisms. The notion of *per-instance differential privacy* formalizes privacy guarantees that vary across data points (Wang, 2019). Several unlearning methods, although not referring explicitly to the term *per-instance*, derive *instance-independent unlearning methods*. Guo et al. (2020) use influence functions to compute Newton-style updates for general convex objectives, with privacy guarantees obtained via objective perturbation. Izzo et al. (2021) derive a projected residual update for linear regression, removing the contribution of the deleted point from the closed-form solution (without privacy

guarantees). While these approaches are explicitly instance-dependent, they rely on parameter-level updates and therefore do not provide a framework for analyzing noisy gradient descent. In contrast, our approach derives per-instance guarantees directly along the optimization trajectory.

Gaussian differential privacy and privacy accounting. Gaussian Differential Privacy (GDP) (Dong et al., 2022) provides a hypothesis-testing-based privacy framework with tight composition rules and sharp conversion to (ε, δ) guarantees. Earlier analyses of Langevin dynamics (Chien et al., 2024; Chourasia et al., 2021; Ryffel et al., 2022) typically relied on Rényi differential privacy, resulting in looser (ε, δ) bounds. More recently, Bok et al. (2024) leverage GDP composition for iterative algorithms with contractive dynamics, yielding sharper privacy accounting. These analyses exploit a form of *privacy amplification by iteration* (Feldman et al., 2018), whereby the repeated application of noisy contractive updates yields strictly stronger guarantees than those derived from worst-case Gaussian composition. We adapt this framework to the unlearning setting by tracking the privacy loss along a combined learn–then–unlearn trajectory with per-instance sensitivity control.

3 Problem Setting

3.1 Regularized Empirical Risk Minimization

We consider supervised learning with a dataset $D = \{(x_j, y_j)\}_{j=1}^n$, where $x_j \in \mathbb{R}^p$ and $y_j \in \mathbb{R}^d$. Given a per-example loss $\ell(\theta; x, y)$ and a regularizer $r(\theta)$, we define the *non-averaged* regularized empirical risk minimization (ERM) objective

$$f_D(\theta) := \sum_{j=1}^n \ell(\theta; x_j, y_j) + \lambda r(\theta), \quad (1)$$

where $\lambda > 0$.

For a designated index $i \in \{1, \dots, n\}$ corresponding to a deletion request, we define the *leave-one-out* objective

$$f_{D^{-i}}(\theta) := \sum_{j \neq i} \ell(\theta; x_j, y_j) + \lambda r(\theta), \quad (2)$$

which corresponds to training on the retain set with the point (x_i, y_i) removed. Throughout the paper, unlearning is understood as transforming a model trained (approximately) with respect to f_D into one whose distribution is close to that obtained by optimizing $f_{D^{-i}}$.

3.2 Certified per-instance unlearning

We briefly recall the standard notion of differential privacy.

Definition 3.1 (Differential Privacy (Dwork et al., 2006)). A randomized algorithm \mathcal{A} is (ε, δ) -differentially private if for any pair of adjacent (e.g. differing from one data point) datasets D, D' and any measurable set S ,

$$\mathbb{P}(\mathcal{A}(D) \in S) \leq e^\varepsilon \mathbb{P}(\mathcal{A}(D') \in S) + \delta.$$

Differential privacy provides a distributional indistinguishability guarantee with respect to the presence or absence of a single data point in the input dataset. Unlearning aims at removing the influence of a designated *forget set* or *forget point* from a trained model. In certified machine unlearning, this is formalized by requiring that the output of the unlearning procedure be statistically indistinguishable from an output that does not depend on the forgotten data.

The dominant formalization in the early literature was introduced by Ginart et al. (2019).

Definition 3.2 $((\varepsilon, \delta)$ -Reference Unlearning (Ginart et al., 2019)). An unlearning algorithm \mathcal{U} satisfies (ε, δ) -reference unlearning if there exists a *reference algorithm* \mathcal{A} such that, for any retain dataset D_r , forget dataset D_f , and any measurable set S ,

$$\mathbb{P}(\mathcal{U}(\mathcal{A}(D), D_r, D_f) \in S) \leq e^\varepsilon \mathbb{P}(\mathcal{A}(D_r) \in S) + \delta,$$

Waerebeke et al., 2025 refer to this definition as *reference unlearning*, as the guarantee is stated relative to an external reference algorithm \mathcal{A} , typically taken to be retraining from scratch on the retain set D_r . As emphasized in subsequent works (e.g., Georgiev et al., 2024, Waerebeke et al., 2025), this definition is unsatisfactory both conceptually and practically, since it depends on the reference algorithm rather than on the unlearning procedure alone.

To avoid this dependence, Sekhari et al. (2021) proposed a stronger definition that instead compares \mathcal{U} to itself on adjacent unlearning scenarios. Concretely, (ε, δ) -unlearning implies (ε, δ) -reference unlearning by taking $\mathcal{A}'(D_r) = \mathcal{U}(\mathcal{A}(D_r), D_r, \emptyset)$, whereas the converse need not hold in general.

Definition 3.3 $((\varepsilon, \delta)$ -Unlearning (Sekhari et al., 2021)). An unlearning algorithm \mathcal{U} satisfies (ε, δ) -unlearning if for a given learning algorithm \mathcal{A} and any retain dataset D_r , forget dataset D_f , and any measurable set S ,

$$\begin{aligned} \mathbb{P}(\mathcal{U}(\mathcal{A}(D), D_r, D_f) \in S) \\ \leq e^\varepsilon \mathbb{P}(\mathcal{U}(\mathcal{A}(D_r), D_r, \emptyset) \in S) + \delta. \end{aligned}$$

The above definition does not depend on the forget set or data point. We specifically focus on the relevant setting where the deletion request targets a *specific data point* and introduce *per-instance unlearning* (see Figure 1 for intuition).

Definition 3.4 $((\varepsilon, \delta)$ -Per-Instance Unlearning). Let \mathcal{A} be a randomized learning algorithm and \mathcal{U} an unlearning algorithm. For a dataset D and a point $(x_i, y_i) \in D$, the algorithm \mathcal{U} satisfies (ε, δ) -per-instance unlearning if for any measurable set S ,

$$\begin{aligned} & \mathbb{P}(\mathcal{U}(\mathcal{A}(D), D^{-i}, (x_i, y_i)) \in S) \\ & \leq e^\varepsilon \mathbb{P}(\mathcal{U}(\mathcal{A}(D^{-i}), D^{-i}, \emptyset) \in S) + \delta \end{aligned}$$

where $D^{-i} := D \setminus \{(x_i, y_i)\}$.

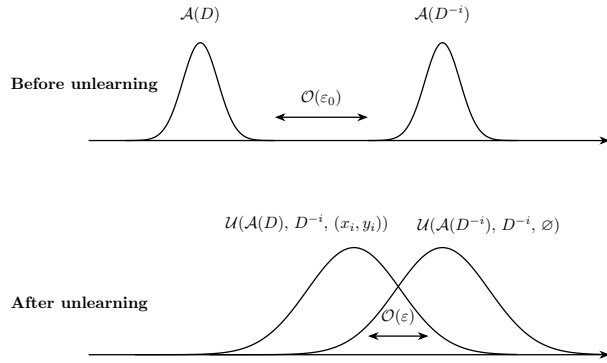


Figure 1: Intuition behind per-instance unlearning. **Top:** After training, the parameter distributions induced by $\mathcal{A}(D)$ and $\mathcal{A}(D^{-i})$ are sharply concentrated and well separated, resulting in a large privacy gap ε_0 . **Bottom:** After applying the unlearning procedure \mathcal{U} , the resulting distributions corresponding to $\mathcal{U}(\mathcal{A}(D), D^{-i}, (x_i, y_i))$ and $\mathcal{U}(\mathcal{A}(D^{-i}), D^{-i}, \emptyset)$ become closer, yielding a much smaller privacy parameter $\varepsilon \ll \varepsilon_0$.

Unlike standard differential privacy, per-instance unlearning tailors its guarantees to the specific data point (x_i, y_i) targeted by the deletion request. The analysis therefore aims to quantify the amount of noise and computation required so that the post-hoc unlearned output matches, in distribution, the outcome that would have been obtained had the point never been included in the training set.

3.3 Algorithms: learn then targeted unlearn

We introduce our learning algorithm \mathcal{A} and unlearning algorithm \mathcal{U} .

Langevin learning \mathcal{A} Given a step size η and an initial noise level σ_{learn} , the discrete Langevin update is

$$\begin{aligned} \theta_{k+1} &= \theta_k - \eta \nabla_\theta f_D(\theta_k) + \sqrt{2\eta\sigma_{\text{learn}}^2} \xi_k, \\ \xi_k &\sim \mathcal{N}(0, I). \end{aligned} \quad (3)$$

After T steps, $\theta_T \sim \mathcal{A}(D)$.

We require $\sigma_{\text{learn}} > 0$ (possibly very small) so that the learning algorithm \mathcal{A} is randomized and induces a non-degenerate output distribution. This randomness is necessary to quantify the privacy loss between training on D and retraining on the retain dataset D^{-i} .

Targeted unlearning \mathcal{U} via retain-set fine-tuning Given an unlearning request for (x_i, y_i) , we run K additional Langevin steps on D^{-i} with calibrated noise level σ_{unlearn} :

$$\begin{aligned} \theta_{k+1} &= \theta_k - \eta \nabla_\theta f_{D^{-i}}(\theta_k) + \sqrt{2\eta\sigma_{\text{unlearn}}^2} \xi_k, \\ \xi_k &\sim \mathcal{N}(0, I). \end{aligned} \quad (4)$$

The output is $\theta_{T+K} \sim \mathcal{U}(\mathcal{A}(D), D^{-i}, (x_i, y_i))$.

4 Theory for Certified Per-instance Unlearning

We track the privacy loss along the optimization trajectory generated by the learning and unlearning algorithms \mathcal{A} and \mathcal{U} (Proposition 4.2). This analysis explicitly reveals how privacy guarantees depend on individual data points, as captured by their *per-instance* sensitivities. Our key contribution is Theorem 4.3, which leverages a high-probability control of these sensitivities to derive (ε, δ) -per-instance unlearning guarantees (in the sense of Definition 3.4) for ridge regression.

4.1 Privacy loss tracking under contractive updates and per-instance sensitivity

We rely on the shifted interpolation framework of Bok et al. (2024) to track privacy loss along the optimization trajectory. This analysis crucially relies on the contraction of the deterministic gradient map associated with Langevin dynamics, which yields privacy amplification by iteration (Feldman et al., 2018). We formalize this requirement in the following assumption.

Assumption 4.1. Both objectives f_D and $f_{D^{-i}}$ are differentiable, m -strongly convex and L -smooth. Under these assumptions, the gradient map $\Phi(\theta) = \theta - \eta \nabla f(\theta)$ is contractive for any step size $0 < \eta < 2/L$, with contraction factor $c = \max\{ |1 - \eta m|, |1 - \eta L| \}$ (Bubeck, 2015; Nesterov, 2004). To ensure a strict contraction ($c < 1$), we fix $\eta = 1/L$, yielding $c = 1 - \eta m < 1$.

Following (Bok et al., 2024), we work within the Gaussian Differential Privacy (GDP) framework. For μ -GDP guarantees, we denote by $\varepsilon_{\text{GDP}}(\mu, \delta)$ the value of ε such that (ε, δ) -differential privacy holds. Formal definitions of GDP and the conversion from μ to (ε, δ) are given in Appendix A.

Compared trajectories for privacy analysis. The analyzed privacy gap is measured between two parameter trajectories $(\theta_k)_{k \geq 0}$ and $(\theta'_k)_{k \geq 0}$ (see Figure 2) initialized at the same deterministic point $\theta_0 = \theta'_0$. The (real) trajectory (θ_k) follows learning algorithm \mathcal{A} on the full dataset D for T iterations with noise level $\sigma_{\text{learn}} > 0$, and K unlearning steps via \mathcal{U} on the retain set D^{-i} with noise level $\sigma_{\text{unlearn}} > 0$. The second trajectory (θ'_k) corresponds to the (theoretical) retraining path, obtained by running the same learning and unlearning procedures directly on D^{-i} .

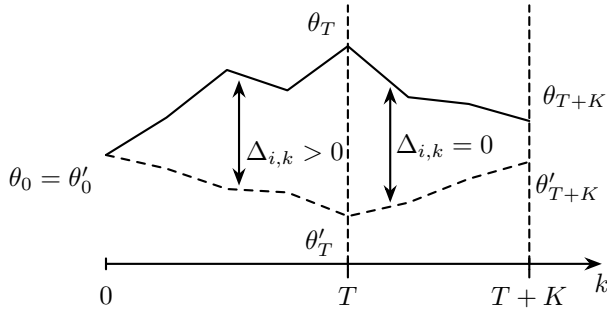


Figure 2: Learn–unlearn vs. retraining trajectories. The solid path (θ_k) corresponds to training on the full dataset D followed by unlearning, while the dashed path (θ'_k) corresponds to (fictitiously) training and retraining on the retain dataset D^{-i} .

Proposition 4.2 (Gaussian DP accounting of the unlearning mechanism \mathcal{U} for bounded per-instance sensitivities). *Consider the two parameter trajectories $(\theta_k)_{k \geq 0}$ and $(\theta'_k)_{k \geq 0}$ defined as above. Assume that Assumption 4.1 holds with contraction factor $c < 1$.*

For an unlearning request concerning (x_i, y_i) , define the per-instance sensitivity at time k as

$$\Delta_{i,k} = \|\eta(\nabla f_{D^{-i}}(\theta_k) - \nabla f_D(\theta_k))\| = \eta \|\nabla \ell(\theta_k; x_i, y_i)\|$$

and assume that there exists a deterministic sequence $\{s_{i,k}\}_{k=0}^T$ (which does not depend on the stochastic trajectory of θ_k) such that $\forall k \leq T$, $\Delta_{i,k} \leq s_{i,k}$.

Then, the final outputs θ_{T+K} and θ'_{T+K} satisfy μ -Gaussian Differential Privacy with parameter μ_{T+K}^i given by,

$$\mu_{T+K}^i = \frac{\sum_{k=0}^T c^{T+K-k} s_{i,k}}{\sqrt{V_{\text{learn}} + V_{\text{unlearn}}}},$$

with

$$V_{\text{learn}} := \sum_{k=0}^T 2\eta\sigma_{\text{learn}}^2 c^{2(T+K-k)},$$

$$V_{\text{unlearn}} := \sum_{k=T+1}^{T+K} 2\eta\sigma_{\text{unlearn}}^2 c^{2(T+K-k)}.$$

In particular, for any $\delta \in (0, 1)$, the unlearning mechanism \mathcal{U} achieves $(\varepsilon_{\text{GDP}}(\mu_{T+K}^i, \delta), \delta)$ -per-instance unlearning (in the sense of Definition 3.4).

4.2 Limits of deterministic sensitivity bounds

Proposition 4.2 relies on deterministic bounds on the per-step sensitivities $\Delta_{i,k}$. In general, such bounds require either the loss gradient to be uniformly bounded, or the loss to be Lipschitz in θ . These assumptions exclude important settings, including standard linear regression. Moreover, when Gaussian noise is used, the iterates θ_k have unbounded support; if the loss gradient is unbounded, this directly implies that $\Delta_{i,k}$ itself cannot be deterministically bounded.

This situation arises naturally in ridge regression trained by Langevin dynamics. In this case, sensitivities are neither uniformly bounded nor deterministic, and their distribution has unbounded support due to the Gaussian nature of the iterates. However, our key contribution in Theorem 4.3 is to exploit the Gaussian structure of the pointwise gradient loss in ridge regression to derive sharp *high-probability* sensitivity bounds and calibrate unlearning noise to the data point to unlearn.

4.3 Certified per-instance unlearning guarantees in the case of Ridge regression

In this section, we consider multi-output linear ridge regression with inputs $X \in \mathbb{R}^{n \times p}$, outputs $Y \in \mathbb{R}^{n \times d}$, and parameter $\theta \in \mathbb{R}^{p \times d}$ with deterministic initialization θ_0 . The objective is

$$f_D(\theta) = \sum_{j=1}^n \frac{1}{2} \|x_j^\top \theta - y_j\|_2^2 + \frac{\lambda}{2} \|\theta\|_F^2,$$

Theorem 4.3 (Certified per-instance unlearning for ridge regression). *Consider the multi-output linear ridge regression setting introduced above, trained with learning algorithm \mathcal{A} and noise $\sigma_{\text{learn}} > 0$ for T iterations. Assume that Assumption 4.1 holds with contraction factor $c < 1$.*

Suppose we want to unlearn a data point (x_i, y_i) in the sense of Definition 3.4 with fixed target privacy level $(\varepsilon, \delta) \in (0, \infty) \times (0, 1)$, and a fixed unlearning horizon $K \geq 1$.

(i) High-probability per-instance sensitivities.

Set $\delta_s \in (0, \delta)$. There exists an explicit, data-dependent sequence $\{s_{i,k}^{\delta_s}\}_{k=0}^T$ such that

$$\mathbb{P}\left(\forall k \leq T, \Delta_{i,k} = \eta \|\nabla \ell(\theta_k; x_i, y_i)\|_F \leq s_{i,k}^{\delta_s}\right) \geq 1 - \delta_s,$$

where each $s_{i,k}^{\delta_s}$ is computable in closed form from $(X, Y, x_i, y_i, \sigma_{\text{learn}}, T)$ via a noncentral χ^2 quantile (see Proposition 4.4).

(ii) Calibration of unlearning noise. Set $\delta_m = \delta - \delta_s$. Then the minimal unlearning noise level which satisfies (ε, δ) -per-instance unlearning of (x_i, y_i) in the sense of Definition 3.4 is defined as

$$\sigma_{\text{unlearn}} := \arg \min_{\sigma \geq 0} \left\{ \sigma : \varepsilon_{\text{GDP}}\left(\mu_i(\sigma), \delta_m\right) \leq \varepsilon \right\},$$

where

$$\mu_i(\sigma) := \frac{\sum_{k=0}^T c^{T+K-k} s_{i,k}^{\delta_s}}{\sqrt{V_{\text{learn}} + V_{\text{unlearn}}(\sigma)}}.$$

V_{learn} and V_{unlearn} are defined in Proposition 4.2.

Proposition 4.4 (High-probability sensitivity bounds $s_{i,k}^{\delta_s}$ for ridge regression). *Consider the multi-output linear ridge regression setting introduced above. Define the data-dependent matrices*

$$M := I_p - \eta(X^\top X + \lambda I_p), \quad B := X^\top Y.$$

For a fixed data point (x_i, y_i) and each iteration $k \geq 0$, the residual $r_{i,k} := x_i^\top \theta_k - y_i \sim \mathcal{N}(\mu_{i,k}, v_{i,k} I_d)$, where

$$\begin{aligned} \mu_{i,k} &:= x_i^\top \left(M^k \theta_0 + \eta \sum_{j=0}^{k-1} M^j B \right) - y_i, \\ v_{i,k} &:= 2\eta\sigma_{\text{learn}}^2 \sum_{j=0}^{k-1} \|(M^j)^\top x_i\|_2^2. \end{aligned}$$

It follows that

$$\frac{\|r_{i,k}\|_2^2}{v_{i,k}} \sim \chi_d'^2 \left(\frac{\|\mu_{i,k}\|_2^2}{v_{i,k}} \right),$$

that is, a non-central chi-square distribution with d degrees of freedom and non-centrality parameter $\|\mu_{i,k}\|_2^2/v_{i,k}$.

As $\Delta_{i,k} = \eta \|x_i\|_2 \|r_{i,k}\|_2$, for any $\delta_s \in (0, 1)$ define

$$s_{i,k}^{\delta_s} := \eta \|x_i\|_2 \sqrt{v_{i,k} q_{i,k}(1 - \frac{\delta_s}{T})},$$

where $q_{i,k}(\cdot)$ denotes the quantile function of the above $\chi_d'^2$ distribution. Then,

$$\mathbb{P}\left(\forall k \leq T, \Delta_{i,k} \leq s_{i,k}^{\delta_s}\right) \geq 1 - \delta_s.$$

Remark 4.5 (Exact unlearning for ridge regression). For ridge regression, exact unlearning is possible when targeting the exact regularized least-squares (LS) solution. In particular, letting $A := X^\top X + \lambda I_p$ and $H := X A^{-1} X^\top$, the leave-one-out (LOO) prediction admits the closed form

$$\hat{y}_i^{(-i)} = \hat{y}_i - \frac{\hat{y}_i - y_i}{1 - (H)_{ii}}, \quad \text{where } \hat{y} = Hy,$$

which follows from the Sherman–Morrison formula (Golub et al., 1979; Hastie et al., 2004).

However, this closed-form expression applies only at the exact LS solution. Using this formula prior to convergence introduces a discrepancy with exact unlearning and, moreover, cannot be safeguarded by a standard DP mechanism to ensure valid privacy guarantees. As a result, the LOO formula does not solve the unlearning problem in the finite-time regime that we consider and offers limited potential for generalization beyond the linear case. From a computational standpoint, applying the LOO formula also requires forming the hat matrix and explicitly inverting the normal matrix A , whose cost and numerical stability degrade rapidly with the dimension p , especially in weakly regularized regimes. While our approach also involves storing the hat matrix, it avoids any matrix inversion and operates directly through iterative updates.

5 Experiments

5.1 Linear setting

In this section, we implement Algorithm 1 (see Appendix D.1), which describes the complete learning and unlearning pipeline.

Task and setup. We consider image classification on MNIST (Lecun et al., 1998) with a fixed-feature pipeline: images are mapped to representations $\phi(x)$ by a frozen ResNet-50 backbone, and only a multi-output ridge regression head ($d = 10$) is trained. Predictions are obtained by taking the arg max over the

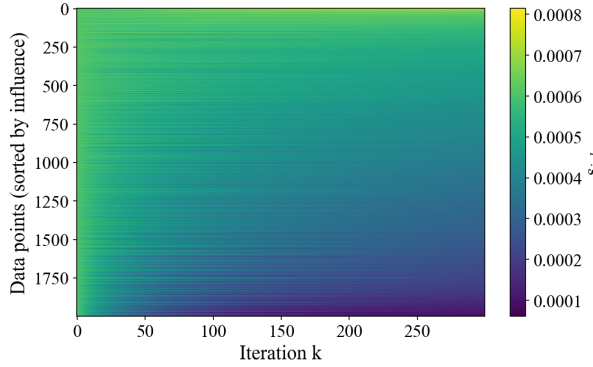


Figure 3: High-probability sensitivity bounds $s_{i,k}^{\delta_s}$ for all MNIST training points in the linear ridge regression setting. Rows correspond to data points and columns to learning iterations. Points are sorted by increasing final sensitivity $s_{i,T}^{\delta_s}$, highlighting substantial per-instance heterogeneity already at the level of analytical bounds.

head outputs. All unlearning operations therefore take place in a linear, strongly convex regime.

Training and unlearning. Learning is performed for $T = 300$ gradient steps on the full dataset D , followed by $K = 30$ additional steps on the reduced dataset D^{-i} to unlearn a single point (see the ablation study on K in Appendix D.2). We use ℓ_2 -regularization with $\lambda = 10^{-4}$ and set the step size to $\eta = 1/L$, so that the gradient map is contractive with factor $c = 1 - m/L$ (Assumption 4.1). Gaussian noise with standard deviation $\sigma_{\text{learn}} = 0.01$ is injected during learning, while the unlearning noise σ_{unlearn} is calibrated to reach a target (ε, δ) guarantee, and we conventionally take $\delta = 1/n$.

Per-instance sensitivity along training. Proposition 4.4 provides, for each training point, a deterministic high-probability bound $\{s_{i,k}^{\delta_s}\}_{k \leq T}$ on its per-step sensitivity. Figure 3 visualizes these bounds for all MNIST training points and reveals pronounced heterogeneity across both points and iterations, indicating that a single uniform sensitivity bound is inherently misleading. We additionally verify that the analytical bounds are not overly conservative by comparing them to empirical sensitivities measured along Langevin training trajectories; see Figure 7 in Appendix.

Selection of points to unlearn. In practice, exhaustively unlearning every data point is computationally prohibitive. Motivated by the heterogeneity revealed in Figure 3, we therefore focus on a small set of representative points spanning different sensitivity regimes. We select 7 indices based on their *difficulty* at convergence, measured by the norm of the

per-sample gradient $\|\nabla_{\theta} \ell(\theta_T; x_i, y_i)\|$ after one full (random) training on D . Points are ranked according to this quantity and we retain the easiest point, the hardest point, and several intermediate quantiles (see Figure 4).

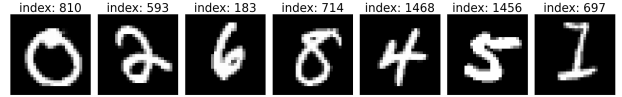


Figure 4: Representative MNIST examples selected for unlearning, ordered from left to right by increasing difficulty, as measured by the per-sample gradient norm $\|\nabla_{\theta} \ell(\theta_T; x_i, y_i)\|$ at convergence for a certain seed.

Privacy–utility trade-off. Figure 5 shows the privacy–utility trade-off induced by unlearning. All curves report test accuracy averaged over 20 independent runs of the learning–unlearning procedure. As expected, stronger privacy guarantees (smaller ε) require injecting more noise and lead to lower accuracy.

Solid lines correspond to *per-instance* unlearning (our method), while dashed lines denote a *uniform* baseline that follows the same contractive optimization dynamics and Gaussian DP accounting but relies on a single global sensitivity bound shared across all points (see Appendix D.2). This uniform calibration assumes oracle knowledge of the maximal gradient magnitude encountered during training and applies the same worst-case noise level to all deletion requests.

As illustrated in Figure 5, per-instance calibration reveals a pronounced heterogeneity in the privacy–utility trade-off. At a fixed privacy budget ε , post-unlearning accuracy varies substantially across removed points, highlighting that the difficulty of unlearning is inherently point-dependent. The uniform baseline fails to adapt to this variability, resulting in overly conservative behavior for most data points. In contrast, per-instance calibration consistently achieves a more favorable privacy–utility trade-off.

Appendix D.2 reports the per-instance unlearning noise levels σ_{unlearn} , which vary by up to a factor of five across data points for a fixed privacy target.

5.2 Non-linear setting

We now turn to a non-linear setting in order to assess whether the heterogeneity observed in the linear case persists for realistic deep learning models.

Model and data. We consider image classification on CIFAR-10 (Krizhevsky and Hinton, 2009). The predictor is a convolutional neural network with a VGG-style architecture, trained end-to-end with

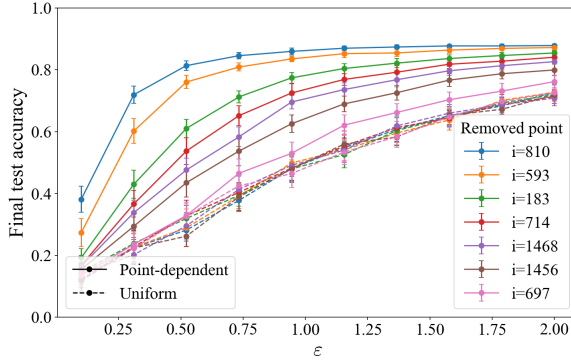


Figure 5: Privacy–utility trade-off on MNIST. Final test accuracy as a function of the privacy budget ε for per-instance unlearning (solid lines) and a uniform baseline (dashed lines). Each curve corresponds to a distinct removed training point, highlighting the heterogeneity of the trade-off across points.

gradient descent. The optimization problem is non-convex and the training dynamics depend strongly on the trajectory.

Training and unlearning. We train for $T = 500$ steps on the dataset D with learning rate $\eta = 10^{-2}$, full batch (to avoid introducing extra randomness from mini-batch sampling), using ℓ_2 -regularization with $\lambda = 10^{-4}$ and full gradient clipping at $C = 1.0$ (as it is a common practice when training neural networks under privacy constraints). Unlearning continues for $K = 20$ steps on D^{-i} . During learning we inject no noise ($\sigma_{\text{learn}} = 0.0$), and, crucially, the *same* Gaussian noise level $\sigma_{\text{unlearn}} = 0.02$ is used for all points during unlearning (no per-point calibration). Although this procedure constitutes a very natural extension of our previous unlearning algorithm to this non-linear setting, it is impossible to certify that Definition 3.4 is satisfied with any level of privacy guarantee. We will thus use below an empirical auditing method to assess the individual privacy guarantees after unlearning.

Representative points. To probe heterogeneity without exhaustively unlearning all samples, we select a small set of representative indices based on an early-training proxy. After 50 noiseless training steps, we compute the pointwise gradient norms $\|\nabla_{\theta} \ell(\theta_{50}; x_i, y_i)\|$ and select indices at fixed quantiles of this distribution, spanning weakly to strongly influential points (see Figure 6). All subsequent unlearning experiments are performed on these fixed indices.

Monte Carlo protocol. To account for the stochasticity induced by the random initialization and the injected Gaussian unlearning noise, the entire unlearning procedure is repeated $R = 50$ times for each index i . All reported quantities are computed



Figure 6: Representative CIFAR-10 samples selected at fixed quantiles of the early-training pointwise gradient norm. These images correspond to the indices used in Table 1.

from the aggregated distributions obtained over these R runs.

Empirical privacy evaluation. For each index i , we compare the distribution of final model parameters obtained by unlearning (x_i, y_i) with the distribution obtained by retraining from scratch on D^{-i} with the same protocol (T steps with no noise $\sigma_{\text{learn}} = 0.0$ and K steps with $\sigma_{\text{unlearn}} = 0.02$). We estimate the corresponding hypothesis-testing trade-off curve $\beta_i(\alpha)$ using a linear distinguisher on the model logits evaluated on a fixed probe set. From the resulting empirical trade-off curve, we fit a Gaussian differential privacy (GDP) parameter μ_i defined by

$$\beta_i(\alpha) \approx \Phi(\Phi^{-1}(1 - \alpha) - \mu_i).$$

We observe that this Gaussian approximation provides a good fit to the empirical trade-off curves across all representative points, supporting the use of GDP as a meaningful empirical summary even in non-convex settings (see Appendix D.3 for quantitative fit diagnostics). For interpretability, we convert each μ_i into an (ε_i, δ) guarantee by fixing $\delta = 1/n$, and numerically inverting the standard GDP-to-DP conversion.

Table 1: Non-linear unlearning on CIFAR-10. Reported values are obtained by aggregating $R = 50$ independent runs per point. All points are unlearned using the same noise level σ_{unlearn} , yet the resulting privacy guarantees ε_i (computed at $\delta = 1/n$) exhibit substantial heterogeneity.

Index i	AUC	$\hat{\mu}_i$	$\hat{\varepsilon}_i$ ($\delta = 1/n$)
358	0.670	0.754	2.05
471	0.764	1.062	3.14
418	0.743	1.017	2.98
381	0.747	1.095	3.26
483	0.822	1.614	5.38
90	0.821	1.384	4.41
226	0.950	2.313	8.69

Key observations. Despite using the *same* unlearning noise for all points, the resulting *effective* privacy guarantees vary substantially across indices.

As shown in Table 1, the fitted GDP parameters $\hat{\mu}_i$ differ significantly across representative points, which translates into a wide range of effective privacy levels $\hat{\varepsilon}_i$ (at $\delta = 1/n$). These results highlight a fundamental limitation of uniform unlearning noise in non-linear models: when the same noise level is applied to all points—an approach that implicitly assumes uniform influence—the resulting privacy guarantees vary substantially and depend on how strongly each data point affects the training trajectory.

6 Conclusion

In this work, we propose a point-dependent view of certified machine unlearning, which allows the noise calibration to depend on the specific data point being removed. We find this perspective particularly relevant, as it leads to a credible unlearning procedure in the ridge regression model, in contrast to uniform worst-case calibration that results in a severe loss of accuracy after unlearning.

Our theoretical guarantees rely on training dynamics exhibiting a form of contraction, which is essential for the trajectory-level GDP accounting. This assumption is satisfied for strongly convex and smooth objectives, such as ridge regression, but generally does not hold for end-to-end deep networks, even when using gradient clipping. This being said, the linear case already corresponds to a concrete and practically relevant use case, since linear models naturally arise when only the final prediction head of a neural network is trained, while the feature extractor is kept fixed.

Despite this theoretical limitation, our experiments on non-linear models reveal large variations in effective privacy levels across data points under identical unlearning noise. In particular, the variability in $\hat{\varepsilon}_i$ values is of the same order of magnitude as the variability observed in per-instance unlearning noise for ridge regression. This suggests that heterogeneous unlearning difficulty is not confined to the convex linear setting and motivates the development of principled per-instance guarantees for more general training dynamics.

Broader Impact

This work contributes to the study of machine unlearning, with the goal of enabling reliable post-hoc data deletion without full retraining. Such capabilities are relevant for privacy regulation compliance, data governance, and user control over personal data in deployed machine learning systems. Overall, we expect this work to support the development of more

accountable and interpretable unlearning mechanisms, rather than enabling new forms of misuse.

References

- Umit Yigit Basaran, Sk Miraj Ahmed, Amit Roy-Chowdhury, and Basak Guler. A certified unlearning approach without access to source data. In *Forty-second International Conference on Machine Learning*, 2025.
- Jinho Bok, Weijie J. Su, and Jason Altschuler. Shifted interpolation for differential privacy. In *Proceedings of the 41st International Conference on Machine Learning*, ICML’24. JMLR.org, 2024.
- Sébastien Bubeck. Convex optimization: Algorithms and complexity. *Found. Trends Mach. Learn.*, 8(3–4):231–357, 2015.
- Yinzhi Cao and Junfeng Yang. Towards making systems forget with machine unlearning. In *2015 IEEE Symposium on Security and Privacy*, pages 463–480, 2015.
- Eli Chien, Haoyu Peter Wang, Ziang Chen, and Pan Li. Langevin unlearning: A new perspective of noisy gradient descent for machine unlearning. In *The Thirty-eighth Annual Conference on Neural Information Processing Systems*, 2024.
- Rishav Chourasia, Jiayuan Ye, and Reza Shokri. Differential privacy dynamics of langevin diffusion and noisy gradient descent. In M. Ranzato, A. Beygelzimer, Y. Dauphin, P.S. Liang, and J. Wortman Vaughan, editors, *Advances in Neural Information Processing Systems*, volume 34, pages 14771–14781. Curran Associates, Inc., 2021.
- Jinshuo Dong, Aaron Roth, and Weijie J. Su. Gaussian differential privacy. *Journal of the Royal Statistical Society Series B: Statistical Methodology*, 84(1):3–37, 02 2022.
- Cynthia Dwork, Frank McSherry, Kobbi Nissim, and Adam Smith. Calibrating noise to sensitivity in private data analysis. In *Theory of Cryptography Conference (TCC)*, pages 265–284. Springer, 2006.
- Vitaly Feldman, Ilya Mironov, Kunal Talwar, and Abhradeep Thakurta. Privacy amplification by iteration. In *2018 IEEE 59th Annual Symposium on Foundations of Computer Science (FOCS)*, page 521–532. IEEE, October 2018.

- Kristian Georgiev, Roy Rinberg, Sung Min Park, Shivam Garg, Andrew Ilyas, Aleksander Madry, and Seth Neel. Attribute-to-delete: Machine unlearning via datamodel matching. *CoRR*, abs/2410.23232, 2024.
- Antonio Ginart, Melody Y. Guan, Gregory Valiant, and James Zou. Making AI forget you: Data deletion in machine learning. In *Advances in Neural Information Processing Systems (NeurIPS)*, 2019.
- Gene H. Golub, Michael Heath, and Grace Wahba. Generalized cross-validation as a method for choosing a good ridge parameter. *Technometrics*, 21(2): 215–223, 1979.
- Chuan Guo, Tom Goldstein, Awni Hannun, and Laurens Van Der Maaten. Certified data removal from machine learning models. In *Proceedings of the 37th International Conference on Machine Learning (ICML)*, volume 119 of *Proceedings of Machine Learning Research*, pages 3832–3842. PMLR, 2020.
- Trevor Hastie, Robert Tibshirani, Jerome Friedman, and James Franklin. The elements of statistical learning: Data mining, inference, and prediction. *Math. Intell.*, 27:83–85, 11 2004.
- Zachary Izzo, Mary Anne Smart, Kamalika Chaudhuri, and James Zou. Approximate data deletion from machine learning models. In *Proceedings of The 24th International Conference on Artificial Intelligence and Statistics (AISTATS)*, volume 130 of *Proceedings of Machine Learning Research*, pages 2008–2016. PMLR, 2021.
- Anastasia Koloskova, Youssef Allouah, Animesh Jha, Rachid Guerraoui, and Sanmi Koyejo. Certified unlearning for neural networks. In *Forty-second International Conference on Machine Learning*, 2025.
- Alex Krizhevsky and Geoffrey Hinton. Learning multiple layers of features from tiny images. Technical Report 0, University of Toronto, Toronto, Ontario, 2009.
- Yann Lecun, Yere Yere, Patrick Haffner, Yoesoep Rachmad, and Leon Bottou. Gradient-based learning applied to document recognition. *Proceedings of the IEEE*, 86:2278 – 2324, 12 1998.
- Linda Lu, Ayush Sekhari, and Karthik Sridharan. System-aware unlearning algorithms: Use lesser, forget faster. In Aarti Singh, Maryam Fazel, Daniel Hsu, Simon Lacoste-Julien, Felix Berkenkamp, Tegan Maharaj, Kiri Wagstaff, and Jerry Zhu, editors, *Proceedings of the 42nd International Conference on Machine Learning*, volume 267 of *Proceedings of Machine Learning Research*, pages 40560–40592. PMLR, 13–19 Jul 2025.
- Bill Marino, Meghdad Kurmanji, and Nicholas D. Lane. Position: Bridge the gaps between machine unlearning and AI regulation. In *The Thirty-Ninth Annual Conference on Neural Information Processing Systems Position Paper Track*, 2025.
- Siqiao Mu and Diego Klabjan. Rewind-to-delete: Certified machine unlearning for nonconvex functions. In *The Thirty-ninth Annual Conference on Neural Information Processing Systems*, 2025.
- Seth Neel, Aaron Roth, and Saeed Sharifi-Malvajerdi. Descent-to-delete: Gradient-based methods for machine unlearning. In Vitaly Feldman, Katrina Ligett, and Sivan Sabato, editors, *Proceedings of the 32nd International Conference on Algorithmic Learning Theory*, volume 132 of *Proceedings of Machine Learning Research*, pages 931–962. PMLR, 16–19 Mar 2021.
- Yurii Nesterov. *Introductory Lectures on Convex Optimization*, volume 87 of *Applied Optimization*. Springer, New York, NY, 2004.
- Théo Ryffel, Francis Bach, and David Pointcheval. Differential Privacy Guarantees for Stochastic Gradient Langevin Dynamics. working paper or preprint, February 2022.
- Ayush Sekhari, Jayadev Acharya, Gautam Kamath, and Ananda Theertha Suresh. Remember what you want to forget: Algorithms for machine unlearning. In *Advances in Neural Information Processing Systems (NeurIPS)*, 2021.
- Nazanin Mohammadi Sepahvand, Anvith Thudi, Berivan Isik, Ashmita Bhattacharyya, Nicolas Papernot, Eleni Triantafillou, Daniel M. Roy, and Gintare Karolina Dziugaite. Leveraging per-instance privacy for machine unlearning. In *Forty-second International Conference on Machine Learning*, 2025.
- Anvith Thudi, Hengrui Jia, Casey Meehan, Ilya Shumailov, and Nicolas Papernot. Gradients look alike: Sensitivity is often overestimated in DP-SGD. In *33rd USENIX Security Symposium (USENIX Security 24)*, pages 973–990, Philadelphia, PA, August 2024. USENIX Association.

Martin Van Waerebeke, Marco Lorenzi, Giovanni Neglia, and Kevin Scaman. When to forget? complexity trade-offs in machine unlearning. In *Forty-second International Conference on Machine Learning*, 2025.

Yu-Xiang Wang. Per-instance differential privacy. *Journal of Privacy and Confidentiality*, 9(1), Mar. 2019.

A Gaussian Differential Privacy

We recall the definition of Gaussian Differential Privacy (GDP) introduced by Dong et al. (2022), together with its conversion to (ε, δ) -differential privacy.

Definition A.1 (Gaussian Differential Privacy (Dong et al., 2022)). For two distributions P and Q , define the *trade-off function* $\mathcal{T}(P, Q) : [0, 1] \rightarrow [0, 1]$ by

$$\mathcal{T}(P, Q)(\alpha) := \inf_{\phi: \mathbb{P}_P(\phi=1) \leq \alpha} \mathbb{P}_Q(\phi = 0),$$

where the infimum ranges over all (possibly randomized) tests ϕ . An algorithm \mathcal{A} satisfies μ -Gaussian Differential Privacy (μ -GDP) if, for any adjacent datasets D, D' ,

$$\mathcal{T}(\text{Law}(\mathcal{A}(D)), \text{Law}(\mathcal{A}(D'))) \geq G(\mu),$$

where $G(\mu)$ is the trade-off function between $\mathcal{N}(0, 1)$ and $\mathcal{N}(\mu, 1)$.

A μ -GDP guarantee implies (ε, δ) -differential privacy for any $\varepsilon > 0$, with

$$\delta = \Phi\left(-\frac{\varepsilon}{\mu} + \frac{\mu}{2}\right) - e^\varepsilon \Phi\left(-\frac{\varepsilon}{\mu} - \frac{\mu}{2}\right), \quad (5)$$

where Φ denotes the standard normal cumulative distribution function. Accordingly, for any $\delta \in (0, 1)$, one can obtain an exact conversion from μ -GDP to (ε, δ) -DP by defining $\varepsilon_{\text{GDP}}(\mu, \delta)$ as the unique value of ε that satisfies (5).

B Proof of Proposition 4.2

We adapt the shifted interpolation framework of Bok et al. (2024) to the learn–unlearn setting.

Setup. Let D and D^{-i} be neighboring datasets differing by a single point i . We consider two trajectories initialized at the same point $\theta_0 = \theta'_0$ and evolving as

$$\theta_{k+1} = \phi(\theta_k) + Z_{k+1}, \quad \theta'_{k+1} = \phi'(\theta'_k) + Z'_{k+1}, \quad k = 0, \dots, T + K,$$

where the deterministic update maps are

$$\phi(\theta) = \begin{cases} \theta - \eta \nabla_\theta f_D(\theta), & k \leq T, \\ \theta - \eta \nabla_\theta f_{D^{-i}}(\theta), & k > T, \end{cases} \quad \phi'(\theta) = \theta - \eta \nabla_\theta f_{D^{-i}}(\theta),$$

and the noise variables satisfy

$$Z_{k+1}, Z'_{k+1} \sim \mathcal{N}(0, 2\eta\sigma_k^2 I), \quad \sigma_k = \begin{cases} \sigma_{\text{learn}}, & k \leq T, \\ \sigma_{\text{unlearn}}, & k > T. \end{cases}$$

By Assumption 4.1, the gradient step $\Phi(\theta) = \theta - \eta \nabla_\theta f(\theta)$ is c -contractive, hence both maps ϕ and ϕ' satisfy

$$\|\phi(\theta) - \phi(\theta')\| \leq c\|\theta - \theta'\|, \quad \|\phi'(\theta) - \phi'(\theta')\| \leq c\|\theta - \theta'\|.$$

During learning ($k \leq T$), the two update maps differ. Recall the per-instance per-step sensitivity:

$$\Delta_{i,k} := \|\phi(\theta_k) - \phi'(\theta_k)\| = \eta \|\nabla_\theta f_D(\theta_k) - \nabla_\theta f_{D^{-i}}(\theta_k)\| = \eta \|\nabla_\theta \ell(\theta_k; x_i, y_i)\|$$

By assumption of the theorem, there exists a deterministic sequence $\{s_{i,k}\}_{k=0}^T$ such that

$$\Delta_{i,k} \leq s_{i,k} \quad \text{for all } k \leq T.$$

During unlearning ($k > T$), the two maps coincide so $\Delta_{i,k} = 0$.

We summarize this via

$$\Delta_{i,k} \leq s_{i,k} \mathbf{1}_{\{k \leq T\}} \quad \text{for all } k \in \{0, \dots, T + K\}. \quad (6)$$

B.1 Shifted interpolation

Following [Bok et al. \(2024\)](#), we introduce the *shifted interpolated process* $\{\tilde{\theta}_k\}_{k=0}^{T+K}$ defined by $\tilde{\theta}_0 = \theta_0 = \theta'_0$ and

$$\tilde{\theta}_{k+1} = \lambda_{k+1}\phi(\theta_k) + (1 - \lambda_{k+1})\phi'(\tilde{\theta}_k) + Z_{k+1}, \quad k = 0, \dots, T + K,$$

where $\lambda_{k+1} \in [0, 1]$ is a shift parameter and we impose $\lambda_{T+K} = 1$, which ensures $\tilde{\theta}_{T+K} = \theta_{T+K}$.

Define the interpolation gap z_k by

$$z_k := \|\theta_k - \tilde{\theta}_k\|,$$

with $z_0 = 0$. We now derive a recursion for z_{k+1} . By definition of the interpolated process and cancellation of the noise terms,

$$z_{k+1} = (1 - \lambda_{k+1})\|\phi(\theta_k) - \phi'(\tilde{\theta}_k)\|.$$

We decompose the difference using the triangle inequality:

$$\|\phi(\theta_k) - \phi'(\tilde{\theta}_k)\| \leq \|\phi(\theta_k) - \phi'(\theta_k)\| + \|\phi'(\theta_k) - \phi'(\tilde{\theta}_k)\|. \quad (7)$$

The first term is bounded by the deterministic trajectory sensitivity (see Equation 6):

$$\|\phi(\theta_k) - \phi'(\theta_k)\| = \Delta_{i,k} \leq s_{i,k} \mathbf{1}_{\{k \leq T\}}.$$

The second term is controlled by the c -contractivity of ϕ' :

$$\|\phi'(\theta_k) - \phi'(\tilde{\theta}_k)\| \leq c\|\theta_k - \tilde{\theta}_k\| = cz_k.$$

Combining the two bounds yields

$$\|\phi(\theta_k) - \phi'(\tilde{\theta}_k)\| \leq cz_k + s_{i,k} \mathbf{1}_{\{k \leq T\}}. \quad (8)$$

Substituting into the expression for z_{k+1} gives

$$z_{k+1} \leq (1 - \lambda_{k+1})(cz_k + s_{i,k} \mathbf{1}_{\{k \leq T\}}). \quad (9)$$

Introduce the associated privacy increment

$$a_{k+1} := \lambda_{k+1}(cz_k + s_{i,k} \mathbf{1}_{\{k \leq T\}}). \quad (10)$$

Equations (9)–(10) imply

$$z_{k+1} = cz_k + s_{i,k} \mathbf{1}_{\{k \leq T\}} - a_{k+1}. \quad (11)$$

B.2 One-step tradeoff bound

We now detail how the one-step privacy increment is obtained, following the shifted interpolation analysis of [Bok et al. \(2024\)](#).

Lemma B.1 (Shifted step lemma ([Bok et al. \(2024\)](#))). *Let ϕ, ϕ' be c -contractive maps. Assume that for two random variables $\theta_k, \tilde{\theta}_k$ we have $\|\theta_k - \tilde{\theta}_k\| \leq z_k$, and that $\|\phi(\theta_k) - \phi'(\theta_k)\| < s_k$ almost surely. Then for any $\lambda_k \in [0, 1]$ and independent Gaussian noises $Z_k, Z'_k \sim \mathcal{N}(0, \sigma^2 I)$,*

$$\mathcal{T}(\lambda\phi(\theta_k) + (1 - \lambda_k)\phi'(\tilde{\theta}_k) + Z, \phi'(\theta'_k) + Z') \geq \mathcal{T}(\tilde{\theta}_k, \theta'_k) \otimes G\left(\frac{\lambda(cz_k + s_k)}{\sigma}\right).$$

Remark B.2 (Remark on the shifted step lemma). In the original formulation of the shifted step lemma in [Bok et al. \(2024\)](#), the authors assume a uniform bound $\|\phi(x) - \phi'(x)\| \leq s$ holding for all x in the entire space. In contrast, in Lemma B.1 we only assume that $\|\phi(\theta_k) - \phi'(\theta_k)\| \leq s_k$ almost surely, where θ_k denotes the random variable governing the current iterate.

This relaxation is justified by the structure of the proof of [Bok et al. \(2024\)](#). Indeed, their argument only involves the random quantity $\|\phi(\theta_k) - \phi'(\theta_k)\|$, and does not require a uniform bound over the entire parameter space. As a result, it is sufficient to control this quantity on the support of the law of θ_k .

A subtle but important technical point concerns the decomposition of $\|\phi(\theta_k) - \phi'(\tilde{\theta}_k)\|$. In the original proof, the authors use

$$\|\phi(\theta_k) - \phi'(\tilde{\theta}_k)\| \leq \|\phi(\theta_k) - \phi(\tilde{\theta}_k)\| + \|\phi(\tilde{\theta}_k) - \phi'(\tilde{\theta}_k)\|.$$

The first term is controlled by $c\|\theta_k - \tilde{\theta}_k\|$ by contractivity of ϕ . However, the second term involves $\tilde{\theta}_k$, the auxiliary process, whose law is not explicitly characterized along the interpolation path, which necessitates a uniform bound on $\|\phi(x) - \phi'(x)\|$.

In our setting, the sensitivity bound is available only along the *real trajectory* θ_k . We therefore rely instead on the alternative decomposition, as in Equation 7,

$$\|\phi(\theta_k) - \phi'(\tilde{\theta}_k)\| \leq \|\phi(\theta_k) - \phi'(\theta_k)\| + \|\phi'(\theta_k) - \phi'(\tilde{\theta}_k)\|.$$

The second term is again controlled by $c\|\theta_k - \tilde{\theta}_k\|$ by contractivity of ϕ' , while the first term depends only on the sensitivity of the update map at the actual iterate θ_k . This allows us to work with bounds that are deterministic but data-dependent, which is precisely the regime required for per-instance certified unlearning.

Application to the dynamics. We apply the shifted step Lemma B.1 at iteration k with

$$\|\phi(\theta_k) - \phi'(\theta_k)\| \leq s_{i,k} \mathbf{1}_{\{k \leq T\}}, \quad \sigma := \sqrt{2\eta}\sigma_k.$$

With $a_{k+1} := \lambda_{k+1}(cz_k + s_{i,k} \mathbf{1}_{\{k \leq T\}})$, the one-step tradeoff increment is

$$\mathcal{T}(\tilde{\theta}_{k+1}, \theta'_{k+1}) \geq \mathcal{T}(\tilde{\theta}_k, \theta'_k) \otimes G\left(\frac{a_{k+1}}{\sqrt{2\eta}\sigma_k}\right).$$

B.3 Composition

Using the identities $\tilde{\theta}_0 = \theta'_0$ (hence $\mathcal{T}(\tilde{\theta}_0, \theta'_0) = 0$) and $\tilde{\theta}_{T+K} = \theta_{T+K}$, we can iterate the composition inequality over $k = 0, \dots, T+K$.

$$\begin{aligned} \mathcal{T}(\theta_{T+K}, \theta'_{T+K}) &= \mathcal{T}(\tilde{\theta}_{T+K}, \theta'_{T+K}) \\ &\geq \mathcal{T}(\tilde{\theta}_{T+K-1}, \theta'_{T+K-1}) \otimes G\left(\sqrt{\frac{a_{T+K}^2}{2\eta\sigma_{T+K-1}^2}}\right) \\ &\geq \mathcal{T}(\tilde{\theta}_0, \theta'_0) \otimes G\left(\sqrt{\sum_{k=0}^{T+K} \frac{a_{k+1}^2}{2\eta\sigma_k^2}}\right) \\ &= G\left(\sqrt{\sum_{k=0}^{T+K} \frac{a_{k+1}^2}{2\eta\sigma_k^2}}\right). \end{aligned} \tag{12}$$

where we used strong composition of Gaussian tradeoff functions.

B.4 Endpoint constraint and optimization

Multiplying (11) by c^{T+K-k} and summing over $k = 0, \dots, T+K$, the terms in z_k telescope. Using $z_0 = 0$ and $z_{T+K} = 0$ (from $\lambda_{T+K} = 1$), we obtain

$$\sum_{k=0}^{T+K} c^{T+K-k} a_{k+1} = \sum_{k=0}^{T+K} c^{T+K-k} s_{i,k} \mathbf{1}_{\{k \leq T\}}.$$

Since $s_{i,k} \mathbf{1}_{\{k \leq T\}} = 0$ for $k > T$, the right-hand side equals

$$N_{T+K}^{(i)} := \sum_{k=0}^T c^{T+K-k} s_{i,k}.$$

To optimize (12), we minimize $\sum_{k=0}^{T+K} a_{k+1}^2 / (2\eta\sigma_k^2)$ subject to the above linear constraint. By Cauchy–Schwarz,

$$\sum_{k=0}^{T+K} \frac{a_{k+1}^2}{2\eta\sigma_k^2} \geq \frac{(N_{T+K}^{(i)})^2}{\sum_{k=0}^{T+K} 2\eta\sigma_k^2 c^{2(T+K-k)}}.$$

Plugging this bound into (12) yields

$$\mathcal{T}(\theta_{T+K}, \theta'_{T+K}) \geq G\left(\frac{N_{T+K}^{(i)}}{\sqrt{\sum_{k=0}^{T+K} 2\eta\sigma_k^2 c^{2(T+K-k)}}}\right).$$

Finally, splitting the denominator into learning and unlearning phases gives

$$\sum_{k=0}^{T+K} 2\eta\sigma_k^2 c^{2(T+K-k)} = V_{\text{learn}} + V_{\text{unlearn}},$$

and therefore

$$\mathcal{T}(\theta_{T+K}, \theta'_{T+K}) \geq G(\mu_{T+K}^i), \quad \mu_{T+K}^i = \frac{N_{T+K}^{(i)}}{\sqrt{V_{\text{learn}} + V_{\text{unlearn}}}}.$$

This concludes the proof. \square

Remark (trajectory sensitivities). The quantities $s_{i,k}$ are deterministic upper bounds on the *trajectory sensitivities*

$$\|\phi_k(\theta_k) - \phi'_k(\theta_k)\|,$$

defined on the support of the iterate θ_k . The proof above only requires such bounds to hold pointwise on $\text{supp}(\text{Law}(\theta_k))$. Deriving explicit expressions or computable upper bounds for $\Delta_{i,k}$ is problem-dependent and is addressed separately.

C Proof of Theorem 4.3

We work in the multi-output linear ridge regression setting of Section 4.3, with $X \in \mathbb{R}^{n \times p}$, $Y \in \mathbb{R}^{n \times d}$, and parameter $\theta \in \mathbb{R}^{p \times d}$. Recall the objective

$$f_D(\theta) = \sum_{j=1}^n \frac{1}{2} \|x_j^\top \theta - y_j\|_2^2 + \frac{\lambda}{2} \|\theta\|_F^2.$$

A direct computation yields

$$\nabla_\theta f_D(\theta) = (X^\top X + \lambda I_p)\theta - X^\top Y =: A\theta - B, \quad A := X^\top X + \lambda I_p, \quad B := X^\top Y.$$

C.1 Langevin dynamics and Gaussian iterates

The learning phase follows the discrete-time Langevin dynamics

$$\theta_{k+1} = M\theta_k + \eta B + \sqrt{2\eta\sigma_{\text{learn}}^2} \Xi_k, \quad M := I_p - \eta A, \quad (13)$$

where $\Xi_k \in \mathbb{R}^{p \times d}$ has i.i.d. columns $\xi_k^{(t)} \sim \mathcal{N}(0, I_p)$, independent across $t \in \{1, \dots, d\}$ and k . We assume a deterministic initialization θ_0 .

Writing $\theta_k = [\theta_k^{(1)} \dots \theta_k^{(d)}]$ column-wise, (13) is equivalent to the d independent recursions

$$\theta_{k+1}^{(t)} = M\theta_k^{(t)} + \eta B^{(t)} + \sqrt{2\eta\sigma_{\text{learn}}^2} \xi_k^{(t)}, \quad t = 1, \dots, d. \quad (14)$$

Lemma C.1 (Gaussian propagation and Kronecker covariance). *For every $k \geq 0$,*

$$\text{vec}(\theta_k) \sim \mathcal{N}(\text{vec}(m_k), I_d \otimes \Sigma_k),$$

where $m_k \in \mathbb{R}^{p \times d}$ and $\Sigma_k \in \mathbb{R}^{p \times p}$ satisfy

$$m_{k+1} = Mm_k + \eta B, \quad m_0 = \theta_0,$$

and

$$\Sigma_{k+1} = M\Sigma_k M^\top + 2\eta\sigma_{\text{learn}}^2 I_p, \quad \Sigma_0 = 0.$$

Proof. Fix $t \in \{1, \dots, d\}$. Since $\theta_0^{(t)}$ is deterministic and (14) is affine with additive Gaussian noise, $\theta_k^{(t)}$ is Gaussian for all k . Taking expectations in (14) gives $\mathbb{E}[\theta_{k+1}^{(t)}] = M\mathbb{E}[\theta_k^{(t)}] + \eta B^{(t)}$, which yields the recursion $m_{k+1} = Mm_k + \eta B$ column-wise.

For covariances, define $\bar{\theta}_k^{(t)} := \theta_k^{(t)} - \mathbb{E}[\theta_k^{(t)}]$. Using independence of $\xi_k^{(t)}$ from the past and $\mathbb{E}[\xi_k^{(t)}] = 0$,

$$\bar{\theta}_{k+1}^{(t)} = M\bar{\theta}_k^{(t)} + \sqrt{2\eta\sigma_{\text{learn}}^2} \xi_k^{(t)}.$$

Thus

$$\text{Cov}(\theta_{k+1}^{(t)}) = M \text{Cov}(\theta_k^{(t)}) M^\top + 2\eta\sigma_{\text{learn}}^2 I_p,$$

and since $\text{Cov}(\theta_0^{(t)}) = 0$ we obtain the stated recursion for $\Sigma_k = \text{Cov}(\theta_k^{(t)})$, which is the same for all t .

Finally, for columns $u \neq t$, the recursions (14) are driven by independent noises $\xi_k^{(u)}$ and $\xi_k^{(t)}$ and share the same deterministic drift; since θ_0 is deterministic, an induction gives $\text{Cov}(\theta_k^{(u)}, \theta_k^{(t)}) = 0$ for all k . Therefore, $\text{Cov}(\text{vec}(\theta_k))$ is block-diagonal with d identical blocks Σ_k , i.e. $\text{Cov}(\text{vec}(\theta_k)) = I_d \otimes \Sigma_k$. \square

C.2 Residual isotropy and high-probability sensitivity control

Fix a point (x_i, y_i) with $x_i \in \mathbb{R}^p$ and $y_i \in \mathbb{R}^d$, and define the residual

$$r_{i,k} := x_i^\top \theta_k - y_i \in \mathbb{R}^d.$$

The per-sample loss is $\ell(\theta; x_i, y_i) = \frac{1}{2}\|x_i^\top \theta - y_i\|_2^2$ and

$$\nabla_\theta \ell(\theta_k; x_i, y_i) = x_i r_{i,k}^\top \in \mathbb{R}^{p \times d}, \quad \|\nabla_\theta \ell(\theta_k; x_i, y_i)\|_F = \|x_i\|_2 \|r_{i,k}\|_2,$$

so the per-step sensitivity is

$$\Delta_{i,k} := \eta \|\nabla_\theta \ell(\theta_k; x_i, y_i)\|_F = \eta \|x_i\|_2 \|r_{i,k}\|_2.$$

Lemma C.2 (Isotropic Gaussian law of the residual). *For every $k \geq 0$, the residual $r_{i,k} := x_i^\top \theta_k - y_i$ is Gaussian with*

$$r_{i,k} \sim \mathcal{N}(\mu_{i,k}, v_{i,k} I_d), \quad \mu_{i,k} := x_i^\top m_k - y_i, \quad v_{i,k} := x_i^\top \Sigma_k x_i.$$

Proof. By Lemma C.1, $\text{vec}(\theta_k)$ is a Gaussian random vector in \mathbb{R}^{pd} with mean $\text{vec}(m_k)$ and covariance $I_d \otimes \Sigma_k$. Using the identity

$$x_i^\top \theta_k = (I_d \otimes x_i^\top) \text{vec}(\theta_k),$$

the residual can be written as

$$r_{i,k} = (I_d \otimes x_i^\top) \text{vec}(\theta_k) - y_i.$$

As an affine transformation of a Gaussian vector, $r_{i,k}$ is Gaussian.

Its mean follows by linearity of expectation:

$$\mathbb{E}[r_{i,k}] = (I_d \otimes x_i^\top) \mathbb{E}[\text{vec}(\theta_k)] - y_i = (I_d \otimes x_i^\top) \text{vec}(m_k) - y_i = x_i^\top m_k - y_i = \mu_{i,k}.$$

Its covariance is obtained by standard covariance propagation for linear maps:

$$\begin{aligned} \text{Cov}(r_{i,k}) &= (I_d \otimes x_i^\top) \text{Cov}(\text{vec}(\theta_k)) (I_d \otimes x_i) \\ &= (I_d \otimes x_i^\top) (I_d \otimes \Sigma_k) (I_d \otimes x_i) \\ &= I_d \otimes (x_i^\top \Sigma_k x_i) = v_{i,k} I_d. \end{aligned}$$

This shows that the residual covariance is isotropic across the d output coordinates. \square

Lemma C.3 (Explicit expressions and efficient recursions for $\mu_{i,k}$ and $v_{i,k}$). *For every $k \geq 0$, the mean and covariance iterates admit the closed forms*

$$m_k = M^k \theta_0 + \eta \sum_{j=0}^{k-1} M^j B, \quad \Sigma_k = 2\eta \sigma_{\text{learn}}^2 \sum_{j=0}^{k-1} M^j (M^j)^\top.$$

Consequently, for any fixed data point (x_i, y_i) ,

$$\mu_{i,k} = x_i^\top \left(M^k \theta_0 + \eta \sum_{j=0}^{k-1} M^j B \right) - y_i, \quad v_{i,k} = 2\eta \sigma_{\text{learn}}^2 \sum_{j=0}^{k-1} \|(M^j)^\top x_i\|_2^2.$$

Moreover, defining the sequence $u_0 = x_i$ and $u_{j+1} = M^\top u_j$, the quantities $(v_{i,k})_{k \leq T}$ are obtained by accumulating the squared norms $\|u_j\|_2^2$, and $(\mu_{i,k})_{k \leq T}$ by projecting the recursion $m_{k+1} = Mm_k + \eta B$ onto x_i at each iteration.

Proof. The expression for m_k follows by unrolling the affine recursion $m_{k+1} = Mm_k + \eta B$ with $m_0 = \theta_0$. Similarly, unrolling the recursion $\Sigma_{k+1} = M\Sigma_k M^\top + 2\eta \sigma_{\text{learn}}^2 I_p$ with $\Sigma_0 = 0$ yields

$$\Sigma_k = 2\eta \sigma_{\text{learn}}^2 \sum_{j=0}^{k-1} M^j (M^j)^\top.$$

Taking the quadratic form along x_i gives

$$v_{i,k} = x_i^\top \Sigma_k x_i = 2\eta \sigma_{\text{learn}}^2 \sum_{j=0}^{k-1} x_i^\top M^j (M^j)^\top x_i = 2\eta \sigma_{\text{learn}}^2 \sum_{j=0}^{k-1} \|(M^j)^\top x_i\|_2^2.$$

Finally, $\mu_{i,k} = x_i^\top m_k - y_i$ follows directly from the definition. \square

By Lemma C.2,

$$z_{i,k} := \frac{r_{i,k}}{\sqrt{v_{i,k}}} \sim \mathcal{N}\left(\frac{\mu_{i,k}}{\sqrt{v_{i,k}}}, I_d\right),$$

hence the normalized squared residual satisfies the noncentral chi-square law

$$\frac{\|r_{i,k}\|_2^2}{v_{i,k}} = \|z_{i,k}\|_2^2 \sim \chi_d'^2\left(\frac{\|\mu_{i,k}\|_2^2}{v_{i,k}}\right).$$

Let $q_{i,k}(\cdot)$ denote the quantile function of this distribution. Fix $\delta_s \in (0, 1)$ and define

$$s_{i,k}^{\delta_s} := \eta \|x_i\|_2 \sqrt{v_{i,k} q_{i,k}\left(1 - \frac{\delta_s}{T}\right)}.$$

Define the event

$$\mathcal{G}_i := \left\{ \forall k \leq T, \Delta_{i,k} \leq s_{i,k}^{\delta_s} \right\}.$$

For each fixed $k \leq T$, by the definition of the quantile,

$$\mathbb{P}\left(\Delta_{i,k} \leq s_{i,k}^{\delta_s}\right) = \mathbb{P}\left(\|r_{i,k}\|_2^2 \leq v_{i,k} q_{i,k}\left(1 - \frac{\delta_s}{T}\right)\right) \geq 1 - \frac{\delta_s}{T}.$$

Therefore, by a union bound,

$$\mathbb{P}(\mathcal{G}_i^c) \leq \sum_{k=0}^T \mathbb{P}\left(\Delta_{i,k} > s_{i,k}^{\delta_s}\right) \leq \sum_{k=0}^T \frac{\delta_s}{T} = \delta_s, \quad \text{hence} \quad \mathbb{P}(\mathcal{G}_i) \geq 1 - \delta_s.$$

C.3 From conditional (ε, δ_m) to unconditional (ε, δ)

Recall the definition of certified per-instance unlearning: a randomized mechanism \mathcal{U} satisfies (ε, δ) -per-instance unlearning for point (x_i, y_i) if for all measurable events S ,

$$\mathbb{P}(\mathcal{U}(\mathcal{A}(D), (x_i, y_i)) \in S) \leq e^\varepsilon \mathbb{P}(\mathcal{U}(\mathcal{A}(D^{-i}), \emptyset) \in S) + \delta \quad (15)$$

On the event \mathcal{G}_i , the learning-phase sensitivities satisfy the deterministic bounds $\Delta_{i,k} \leq s_{i,k}^{\delta_s}$ for all $k \leq T$. By Proposition 4.2, this implies the *conditional* (ε, δ_m) guarantee: for all measurable S ,

$$\mathbb{P}(\mathcal{U}(\mathcal{A}(D), (x_i, y_i)) \in S \mid \mathcal{G}_i) \leq e^\varepsilon \mathbb{P}(\mathcal{U}(\mathcal{A}(D^{-i}), \emptyset) \in S \mid \mathcal{G}_i) + \delta_m. \quad (16)$$

We now remove the conditioning. For any measurable S , by the law of total probability,

$$\mathbb{P}(\mathcal{U}(\mathcal{A}(D), (x_i, y_i)) \in S) = \mathbb{P}(\mathcal{U}(\mathcal{A}(D), (x_i, y_i)) \in S \mid \mathcal{G}_i) \mathbb{P}(\mathcal{G}_i) + \mathbb{P}(\mathcal{U}(\mathcal{A}(D), (x_i, y_i)) \in S \mid \mathcal{G}_i^c) \mathbb{P}(\mathcal{G}_i^c) \quad (17)$$

$$\leq \mathbb{P}(\mathcal{U}(\mathcal{A}(D), (x_i, y_i)) \in S \mid \mathcal{G}_i) \mathbb{P}(\mathcal{G}_i) + \delta_s, \quad (18)$$

since $\mathbb{P}(\mathcal{U}(\mathcal{A}(D), (x_i, y_i)) \in S \mid \mathcal{G}_i^c) \leq 1$ and $\mathbb{P}(\mathcal{G}_i^c) \leq \delta_s$.

Combining (18) with (16) yields

$$\begin{aligned} \mathbb{P}(\mathcal{U}(\mathcal{A}(D), (x_i, y_i)) \in S) &\leq (e^\varepsilon \mathbb{P}(\mathcal{U}(\mathcal{A}(D^{-i}), \emptyset) \in S \mid \mathcal{G}_i) + \delta_m) \mathbb{P}(\mathcal{G}_i) + \delta_s \\ &\leq e^\varepsilon \mathbb{P}(\mathcal{U}(\mathcal{A}(D^{-i}), \emptyset) \in S \mid \mathcal{G}_i) \mathbb{P}(\mathcal{G}_i) + \delta_m \mathbb{P}(\mathcal{G}_i) + \delta_s, \\ &\leq e^\varepsilon \mathbb{P}(\mathcal{U}(\mathcal{A}(D^{-i}), \emptyset) \in S) + \delta_m + \delta_s, \end{aligned}$$

where we used $\mathbb{P}(\mathcal{U}(\mathcal{A}(D^{-i}), \emptyset) \in S \mid \mathcal{G}_i) \mathbb{P}(\mathcal{G}_i) = \mathbb{P}(\mathcal{U}(\mathcal{A}(D^{-i}), \emptyset) \in S)$ and $\mathbb{P}(\mathcal{G}_i) \leq 1$. This proves (15) with $\delta = \delta_m + \delta_s$. This concludes the proof of Theorem 4.3.

D Implementation details

D.1 Learning, calibration, and targeted unlearning

Combining Theorem 4.3 and Proposition 4.4 yields an explicit and fully implementable procedure for per-instance Langevin unlearning in the case of ridge regression. Algorithm 1 summarizes the complete pipeline.

D.2 Implementation details for MNIST experiments

Dataset and splits. We use the MNIST dataset, consisting of 60,000 training images and 10,000 test images of handwritten digits in 10 classes. Rather than training on the full dataset, we deliberately work with a *restricted training set size* $n = 2000$. This choice is intentional: in certified unlearning and privacy accounting, guarantees typically improve with larger datasets, and we aim to avoid reporting favorable results that are driven primarily by a large sample size. Using a moderate value of n highlights the effect of per-instance sensitivity heterogeneity rather than a trivial scaling effect in n .

We first extract features from 6000 training images and 1000 test images, then concatenate them and randomly select $n = 2000$ points for training. All remaining points are used for test. The split is performed once using a fixed random permutation.

Feature extraction. Each MNIST image is mapped to a fixed feature representation using a ResNet-50 network pre-trained on ImageNet. The backbone is kept frozen throughout all experiments. Images are resized to 224×224 , converted to three channels, and normalized using the standard ImageNet mean and variance. We remove the final fully connected layer and extract the output of the global average pooling layer, yielding a feature vector of dimension 2048.

Algorithm 1 Learning, per-instance calibration, and targeted Langevin unlearning for ridge regression

Input: dataset $D = \{(x_j, y_j)\}_{j=1}^n$, deletion index i , learning horizon T , unlearning horizon K , step size η , regularization λ , strong convexity m , learning noise σ_{learn} , target privacy (ε, δ) , sensitivity tail probability δ_s , initial parameter θ_0 .

Output: unlearned parameter θ_{T+K} , calibrated noise σ_{unlearn} .

Precomputation. Set

$$A = X^\top X + \lambda I, \quad M = I - \eta A, \quad B = X^\top Y.$$

Analytic residual statistics. Compute $(\mu_{i,k}, v_{i,k})_{k=1}^T$ using the closed-form recursions of Lemma C.3, without simulating the Langevin trajectory.

Learning phase (full dataset). Initialize $\theta \leftarrow \theta_0$.

for $k = 1$ **to** T **do**

 Perform one Langevin step on D :

$$\theta \leftarrow \theta - \eta \nabla_\theta f_D(\theta) + \sqrt{2\eta} \sigma_{\text{learn}} \xi_k, \quad \xi_k \sim \mathcal{N}(0, I).$$

 Compute the high-probability sensitivity bound

$$s_{i,k}^{\delta_s} = \eta \|x_i\|_2 \sqrt{v_{i,k} q_{i,k} \left(1 - \frac{\delta_s}{T}\right)},$$

 where $q_{i,k}$ is the quantile of $\chi_d'^2(\|\mu_{i,k}\|_2^2 / v_{i,k})$.

end for

Set $s_{i,k}^{\delta_s} \leftarrow 0$ for $k = T+1, \dots, T+K$. Store $\theta_T \leftarrow \theta$.

Noise calibration (GDP accounting). Let $c = 1 - \eta m$ and define

$$\mu(\sigma) = \frac{\sum_{k=1}^T c^{T+K-k} s_{i,k}^{\delta_s}}{\sqrt{\sum_{k=1}^T 2\eta\sigma_{\text{learn}}^2 c^{2(T+K-k)} + \sum_{k=T+1}^{T+K} 2\eta\sigma^2 c^{2(T+K-k)}}}.$$

Find the smallest σ_{unlearn} such that the GDP-to-DP conversion at level $\delta_m = \delta - \delta_s$ satisfies

$$\varepsilon_{\text{GDP}}(\mu(\sigma_{\text{unlearn}}), \delta_m) \leq \varepsilon.$$

Targeted unlearning (dataset D^{-i}). Initialize $\theta \leftarrow \theta_T$.

for $k = 1$ **to** K **do**

 Perform one Langevin step on D^{-i} :

$$\theta \leftarrow \theta - \eta \nabla_\theta f_{D^{-i}}(\theta) + \sqrt{2\eta} \sigma_{\text{unlearn}} \xi_k, \quad \xi_k \sim \mathcal{N}(0, I).$$

end for

return $\theta_{T+K} \leftarrow \theta$, σ_{unlearn} .

Labels and linear head. Targets are encoded as one-hot vectors in \mathbb{R}^{10} . We train a multi-output linear ridge regression head on top of the frozen features, resulting in a parameter matrix $\theta \in \mathbb{R}^{p \times d}$ with $d = 10$ outputs. A bias term is included by appending a constant feature to each input vector, so that the final input dimension is $p = 2049$.

Randomness and reproducibility. All experiments use fixed random seeds for NumPy and PyTorch. Data ordering is fixed and no data augmentation is applied. The ResNet-50 backbone is evaluated in deterministic inference mode. All reported results are therefore fully reproducible given the same random seed and hardware configuration.

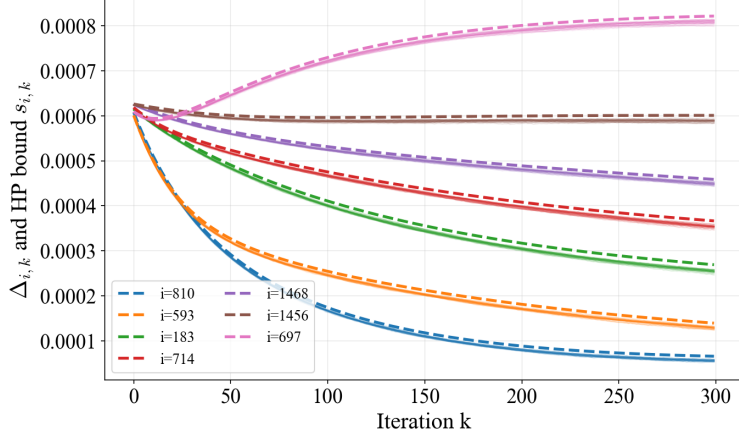


Figure 7: Empirical per-step sensitivities $\Delta_{i,k}$ (transparent solid lines, multiple Langevin runs) versus the corresponding high-probability bounds $s_{i,k}^{\delta_s}$ (dashed) for several representative points (MNIST) and $\sigma_{\text{learn}} = 0.01$. The bounds uniformly dominate the observed trajectories and capture their heterogeneous temporal profiles.

Sanity check: empirical sensitivities vs. high-probability bounds. We compare the empirical per-step sensitivities $\Delta_{i,k} = \eta \|\nabla_{\theta} \ell(\theta_k; x_i, y_i)\|_F$ measured along independent Langevin training trajectories to the corresponding high-probability bounds $s_{i,k}^{\delta_s}$ from Proposition 4.4. Figure 7 shows that the bounds dominate the observed sensitivities across iterations for representative points, while remaining of the correct order of magnitude.

Uniform baseline and sensitivity control. A natural approach for controlling sensitivity in the uniform baseline would be to enforce a global bound via *pointwise* gradient clipping, as commonly done in DP-SGD. However, this choice is incompatible with our analysis. Without clipping, the gradient update associated with an m -strongly convex and L -smooth empirical risk $f(\theta) = \frac{1}{n} \sum_{i=1}^n \ell_i(\theta)$ defines a contractive map

$$\Phi(\theta) = \theta - \eta \nabla f(\theta), \quad \|\Phi(\theta) - \Phi(\theta')\| \leq c \|\theta - \theta'\|, \quad c < 1,$$

for $\eta = 1/L$. With pointwise gradient clipping, the update becomes

$$\Phi_{\text{pw}}(\theta) = \theta - \eta \frac{1}{n} \sum_{i=1}^n \frac{\nabla \ell_i(\theta)}{\max\{1, \|\nabla \ell_i(\theta)\|/C\}},$$

which replaces the gradient of f by an average of *projected* gradients. Although each clipping operator is non-expansive, the resulting map is no longer the gradient of a smooth objective and does not admit a uniform contraction factor. In particular, when different samples enter and leave the clipped regime across iterations, the Jacobian of Φ_{pw} involves a sum of data-dependent projections whose spectral norm cannot be bounded uniformly by a constant strictly smaller than one. As a consequence, no global contraction guarantee can be established, even when all losses ℓ_i are strongly convex and smooth, which breaks the trajectory-level privacy amplification mechanism required for GDP tracking.

To preserve contractivity and enable a consistent comparison, we therefore adopt a different strategy for the uniform baseline. Rather than clipping, we monitor pointwise gradient norms along the training trajectories and fix a single global sensitivity bound equal to their empirical supremum ($C = 1.3$ for MNIST), which is never violated across all of our experiments and random seeds. Importantly, this choice corresponds to the tightest uniform sensitivity bound that can be obtained *for this dataset and this optimization procedure*, and should be viewed as the best-case uniform calibration one could hope for under full knowledge of the optimization trajectories. As such, it relies on *a posteriori* information and constitutes an optimistic, oracle-like calibration that deliberately favors the uniform baseline.

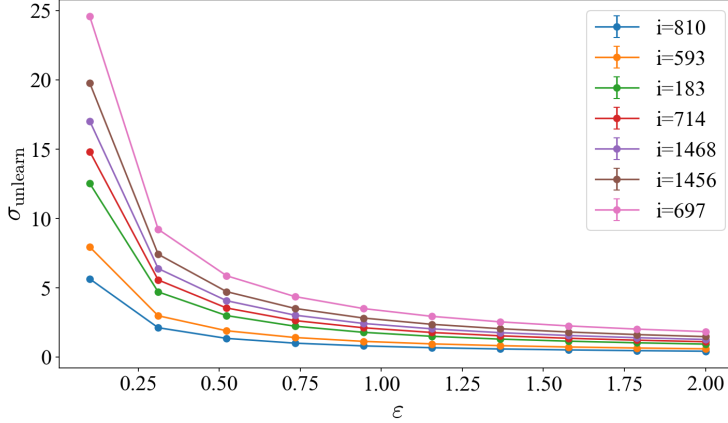


Figure 8: Required unlearning noise level σ_{unlearn} as a function of the target privacy budget ε for several individual removal requests (MNIST). Each curve corresponds to a distinct unlearned data point. For a fixed privacy target, the required noise varies substantially across points, with differences of up to a factor five between the least and most influential examples.

Per-instance unlearning noise calibration. In addition to final test accuracy, we report in Figure 8 the values of the unlearning noise level σ_{unlearn} required to achieve a target privacy budget ε for individual data points. Each curve corresponds to a distinct removal request, and illustrates how the noise calibration varies across points. We highlight the magnitude of this heterogeneity: for a fixed privacy level ε , the required σ_{unlearn} can differ by a factor of up to five between the least and most influential points. This variability persists across the entire range of privacy budgets considered.

Ablation on the unlearning budget K . The unlearning horizon K determines the computational budget of the post-hoc fine-tuning phase on the retain set D^{-i} . At fixed privacy target (ε, δ) , increasing K affects the privacy accounting through additional contraction in the GDP analysis, while distributing the unlearning noise budget over a larger number of iterations. To isolate this effect, we fix ε and vary K , focusing exclusively on the point-dependent unlearning mechanism.

Figure 9 reports the final test accuracy after targeted unlearning at fixed $\varepsilon = 1$ as a function of K , for several representative deletion points. Results are aggregated over multiple random seeds and shown as mean \pm standard deviation. We observe that increasing K generally improves utility up to a plateau, beyond which additional unlearning steps yield diminishing returns. For such points, further accuracy gains cannot be achieved by increasing K alone and instead require relaxing the privacy constraint, i.e., allowing for a larger privacy budget ε .

D.3 CIFAR-10: non-linear unlearning and empirical privacy evaluation

Dataset and splits. We use the CIFAR-10 dataset, consisting of 50,000 training images and 10,000 test images of size 32×32 in 10 classes. As in the MNIST experiments, we deliberately restrict the effective training set size and use only $n = 500$ training points. This choice is intentional: privacy and unlearning guarantees typically improve with larger datasets, and we aim to avoid reporting favorable results driven primarily by dataset size rather than by the behavior of the unlearning mechanism itself. Working with a small n highlights the intrinsic difficulty of targeted unlearning in non-linear models.

We first subsample 5000 images from the CIFAR-10 training split and 1000 images from the test split, concatenate them, and then randomly select $n = 500$ points for training. All remaining samples are used for test. The split is performed once using a fixed random permutation.

Preprocessing and data augmentation. Images are normalized using the standard CIFAR-10 channel-wise mean and standard deviation. For training, we apply random cropping with padding and random

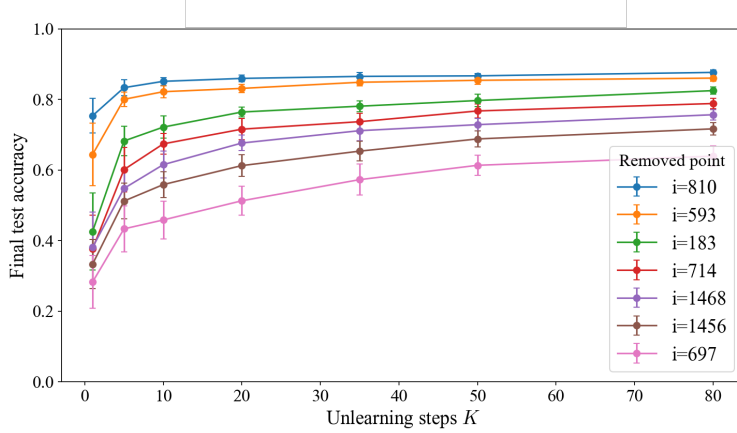


Figure 9: Effect of the unlearning horizon K at fixed privacy level $\varepsilon = 1$ on the final test accuracy (MNIST). Each curve corresponds to a distinct unlearned data point. Larger K improves utility by distributing the unlearning noise over more iterations and increasing contraction, until a point-dependent plateau is reached.

horizontal flips, followed by normalization. No additional data augmentation is used. All preprocessing operations are fixed once the random seed is set.

Model architecture. We use a small VGG-style convolutional neural network tailored to CIFAR-10. The architecture consists of three convolutional blocks, each composed of two 3×3 convolutional layers with ReLU activations, followed by max-pooling. The convolutional backbone is followed by a fully connected classifier with one hidden layer of dimension 256 and dropout. Dropout is used to improve optimization stability in the small-sample regime. All model parameters are trainable.

Training and unlearning protocol. The network is trained using gradient descent with explicit ℓ_2 regularization and optional isotropic Gaussian gradient noise. Training proceeds for T iterations on the full dataset D . Targeted unlearning is performed by continuing optimization for K additional iterations on the retain set D^{-i} .

Empirical trade-off evaluation. Since no closed-form privacy accounting is available for the non-linear setting, we evaluate unlearning guarantees empirically by estimating the privacy trade-off curve between unlearned and retrained models. For each index i , we repeat the following experiment R times with independent random seeds: we train the model on D , unlearn point i using the specified protocol, and independently retrain the model on D^{-i} . This yields two empirical distributions over final model parameters, denoted P_i (unlearned) and Q_i (retrained).

Model representations and distinguisher. To compare P_i and Q_i , we embed each trained model into a finite-dimensional representation by evaluating its logits on a fixed probe set, which is sampled once and shared across all indices and runs. A linear classifier is then trained to distinguish between samples drawn from P_i and Q_i , yielding a scalar score that approximates a log-likelihood ratio.

Empirical trade-off curves and interpretable metrics. From the distinguisher scores, we construct an empirical trade-off curve $\beta_i(\alpha)$, where α and β denote type-I and type-II errors, respectively. In addition to the full trade-off curve, we report the area under the ROC curve (AUC) (see Table 1), which provides a sanity check on the distinguishability between P_i and Q_i ; larger AUC values indicate that the two distributions are more easily distinguishable by the chosen test, while values close to 0.5 correspond to near-indistinguishability.

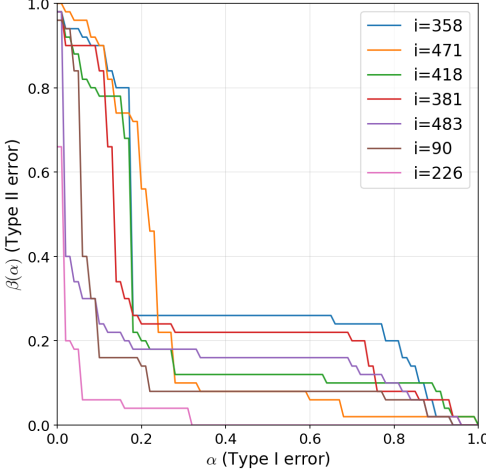


Figure 10: Empirical hypothesis-testing trade-off curves $\beta_i(\alpha)$ for several representative CIFAR-10 points. All points are unlearned using the same noise level $\sigma_{\text{unlearn}} = 0.02$, yet the resulting trade-off profiles differ substantially across indices.

Gaussian DP approximation. To obtain a low-dimensional and interpretable summary of the empirical trade-off curves, we fit for each index i a Gaussian differential privacy (GDP) parameter $\hat{\mu}_i$ by least-squares regression of the form

$$\beta_i(\alpha) \approx \Phi(\Phi^{-1}(1 - \alpha) - \mu_i),$$

where Φ denotes the standard normal cumulative distribution function.

The quality of the approximation is assessed by the mean squared error (MSE) between the fitted GDP curve and the empirical trade-off curve. Across all evaluated indices, the fit error is consistently small (typically between 10^{-3} and 10^{-2}), indicating that GDP provides an accurate approximation of the empirical hypothesis-testing behavior, despite the non-convex and non-linear nature of the training dynamics.

Empirical ε_i at fixed δ . For interpretability and comparison with standard privacy notions, each fitted $\hat{\mu}_i$ is converted into an empirical (ε_i, δ) guarantee by fixing $\delta = 1/n$, where n denotes the number of training points. The corresponding ε_i values are obtained by numerically inverting the standard GDP-to-DP conversion.

We stress that these ε_i values are *empirical* and do not constitute certified guarantees. They should be interpreted as quantitative summaries of distinguishability between unlearned and retrained models under the chosen experimental protocol. Nevertheless, they provide a meaningful way to compare the relative difficulty of unlearning different data points.

E Additional experiments

We include additional experiments on CIFAR-10 and Fashion-MNIST using the same ridge regression setting as MNIST. These experiments reveal comparable privacy–accuracy tradeoffs, with clear per-instance effects.

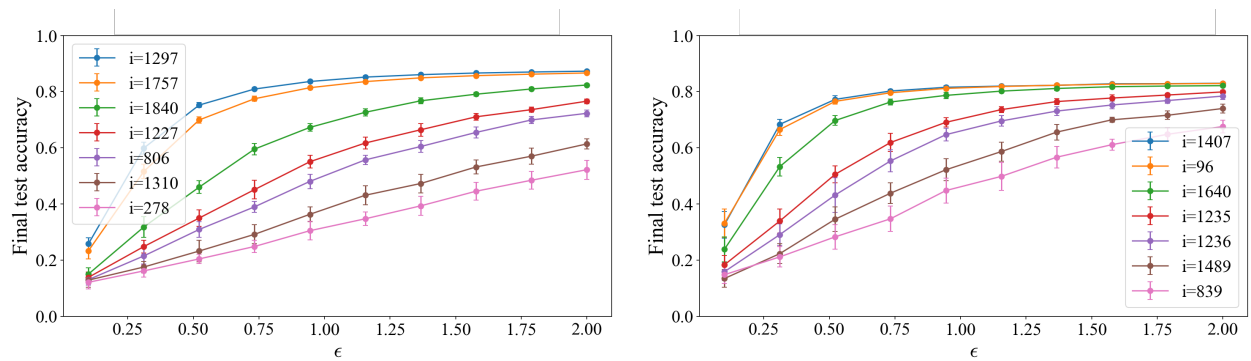


Figure 11: Privacy–utility trade-off for 7 representative points. **Left:** CIFAR-10. **Right:** Fashion-MNIST.